



Application of a metric for complex polynomials to bounded modification of planar Pythagorean-hodograph curves

Rida T. Farouki^a, Marjeta Knez^{b,c,*}, Vito Vitrih^{d,e}, Emil Žagar^{b,c}

^a Mechanical & Aerospace Engineering, University of California, Davis, CA 95616, USA

^b Faculty of Mathematics and Physics, University of Ljubljana, Jadranska 19, Ljubljana, Slovenia

^c Institute of Mathematics, Physics and Mechanics, Jadranska 19, Ljubljana, Slovenia

^d Faculty of Mathematics, Natural Sciences and Information Technologies, University of Primorska, Glagoljaška 8, Koper, Slovenia

^e Andrej Marušič Institute, University of Primorska, Muzejski trg 2, Koper, Slovenia

ARTICLE INFO

MSC:

65D05

65D07

65D17

Keywords:

Complex polynomial

Inner product

Norm

Metric

Pythagorean-hodograph curve

Bounded modification

ABSTRACT

By interpreting planar polynomial curves as complex-valued functions of a real parameter, an inner product, norm, metric function, and the notion of orthogonality may be defined for such curves. This approach is applied to the complex pre-image polynomials that generate planar Pythagorean-hodograph (PH) curves, to facilitate the implementation of bounded modifications of them that preserve their PH nature. The problems of bounded modifications under the constraint of fixed curve end points and end tangent directions, and of increasing the arc length of a PH curve by a prescribed amount, are also addressed.

1. Introduction

In the complex model [1] for planar PH curves, points (x, y) in the Euclidean plane are identified with the complex values $x + iy$. A planar PH curve $\mathbf{r}(t)$ for $t \in [0, 1]$ may be generated from a complex *pre-image polynomial* $\mathbf{w}(t)$ by integrating the hodograph expression $\mathbf{r}'(t) = \mathbf{w}(t)$. This guarantees that the components of $\mathbf{r}'(t) = x'(t) + iy'(t)$ satisfy [2] the polynomial Pythagorean condition

$$x'^2(t) + y'^2(t) = \sigma^2(t),$$

where $\sigma(t) = |\mathbf{r}'(t)| = |\mathbf{w}(t)|^2$ is the *parametric speed* of $\mathbf{r}(t)$ — the derivative ds/dt of the curve arc length s with respect to the parameter t .

Planar PH curves admit an exact computation of quantities such as arc lengths and offset curves [3], that necessitate use of numerical approximation for “ordinary” polynomial curves. However, their non-linear nature entails more sophisticated construction algorithms, and renders *a posteriori* shape modification a difficult task. To address this latter problem, it is important to first formulate a measure of “how close” two PH curves are, i.e., to specify a *metric* for the space of all planar PH curves.

There are several different possible ways to measure the distance between two planar curves. The standard measure is the Hausdorff distance — a distance measure between two curves considered as sets of points in \mathbb{R}^2 . However, one can find examples of curves that have a small Hausdorff distance but are still very different. Another measure is the Fréchet distance, which avoids

* Corresponding author at: Faculty of Mathematics and Physics, University of Ljubljana, Jadranska 19, Ljubljana, Slovenia.

E-mail addresses: farouki@ucdavis.edu (R.T. Farouki), marjetka.knez@mf.uni-lj.si (M. Knez), vito.vitrih@upr.si (V. Vitrih), emil.zagar@mf.uni-lj.si (E. Žagar).

<https://doi.org/10.1016/j.cam.2024.116235>

Received 15 February 2024; Received in revised form 14 June 2024

Available online 28 August 2024

0377-0427/© 2024 The Author(s). Published by Elsevier B.V. This is an open access article under the CC BY-NC-ND license (<http://creativecommons.org/licenses/by-nc-nd/4.0/>).

the aforementioned issue with the Hausdorff distance but is, in general, more complicated to compute [4–6]. A particular Fréchet distance was considered in [7].

Although a polynomial PH curve can be expressed in Bézier form, it is difficult to modify it using its control polygon, since any perturbation of the control polygon will typically yield a non-PH curve. In the case of planar quintic PH curves, one can freely choose two of the five control-polygon legs, the remaining three being expressed in terms of the chosen legs and the roots of a quadratic or quartic equation [8]. Another method of controlling a planar PH curve is by the Gauss–Legendre (or rectifying) control polygon, introduced in [9]. This scheme always generates a PH curve for any rectifying polygon, but there exist multiple PH curves for a given polygon. A simple scheme to select the best curve among the multitude of these PH curves was proposed in [10]. Recently, a complete classification of PH quintics with respect to their global shape has been considered in [11], and this may help understand the possible modifications of planar quintic PH curves. In [12], the problem of identifying the planar quintic PH curve “closest” to a given Bézier curve, that has the same endpoints (and possibly also end tangents), has been analyzed. The distance measure used in this context is based on the sum of the squared differences between pairs of corresponding control points of the two curves.

The complex representation of planar PH curves offers another possible means of efficiently measuring the distance between two PH curves, in terms of the standard concepts of inner products and norms from functional analysis [13]. By introducing a bound on the distance between an original and modified pre-image polynomial, it is possible to characterize the set of changes to its coefficients that define the shape modifications to a planar PH curve that do not compromise its PH nature. The focus of the methodology presented herein is on the planar PH curves, although the approach may be adaptable to the spatial PH curves [14,15] and the many other formulations of PH curves with distinctive properties that have been proposed (see [3] and references therein).

The remainder of this paper is organized as follows. Section 2 introduces the basic concepts of an *inner product*, *norm*, and *metric* for the space of all polynomials in a real variable $t \in [0, 1]$ with complex coefficients. Section 3 then shows that this metric allows an *angle* between such polynomials to be defined, and gives examples of *orthogonal* plane curves specified as complex polynomial functions of a real parameter. Section 4 discusses the application of these concepts to planar PH curves, and it is observed that to maintain the PH nature, modifications should be made to the pre-image polynomial instead of directly to the curve. Modifications satisfying a prescribed bound on the distance between the original and modified pre-image polynomials are discussed in Section 5, and modifications that preserve the end tangents or end points of PH curves are also formulated. Section 6 shows how complex polynomials orthogonal to a specified pre-image polynomial may be used to modify PH curve arc lengths. Finally, Section 7 summarizes the contributions of this study and suggests further possible avenues of investigation.

2. Metric space of complex polynomials

We begin by reviewing some elementary concepts from functional analysis — inner products, norms, and metrics (see [13] for a thorough treatment).

Definition 1. Let $\mathbf{u}(t), \mathbf{v}(t) \in \mathbb{C}[t]$ be complex polynomials in the real variable $t \in [0, 1]$. Their complex-valued *inner product* is defined by

$$\langle \mathbf{u}, \mathbf{v} \rangle = \int_0^1 \mathbf{u}(t) \bar{\mathbf{v}}(t) dt.$$

Definition 2. For any complex polynomial $\mathbf{w}(t) \in \mathbb{C}[t]$, the above inner product induces a norm specified by

$$\|\mathbf{w}\| = \sqrt{\langle \mathbf{w}, \mathbf{w} \rangle}. \tag{1}$$

A metric, or *distance function* on $\mathbb{C}[t]$, can be defined in terms of the norm (1) as

$$\text{distance}(\mathbf{u}, \mathbf{v}) = \|\mathbf{u} - \mathbf{v}\|. \tag{2}$$

Since

$$\begin{aligned} \|\mathbf{u} - \mathbf{v}\|^2 &= \int_0^1 (\mathbf{u}(t) - \mathbf{v}(t))(\bar{\mathbf{u}}(t) - \bar{\mathbf{v}}(t)) dt \\ &= \int_0^1 |\mathbf{u}(t)|^2 + |\mathbf{v}(t)|^2 - 2 \operatorname{Re}(\mathbf{u}(t)\bar{\mathbf{v}}(t)) dt \\ &= \|\mathbf{u}\|^2 + \|\mathbf{v}\|^2 - 2 \operatorname{Re}(\langle \mathbf{u}, \mathbf{v} \rangle), \end{aligned}$$

we have

$$\text{distance}(\mathbf{u}, \mathbf{v}) = \sqrt{\|\mathbf{u}\|^2 + \|\mathbf{v}\|^2 - 2 \operatorname{Re}(\langle \mathbf{u}, \mathbf{v} \rangle)}.$$

Note that $\text{distance}(\mathbf{u}, \mathbf{v}) = 0$ if and only if $\mathbf{u}(t) \equiv \mathbf{v}(t)$. The metric (2) can define the distance between planar curves.

Definition 3. Let $\mathbf{r}(t)$ and $\mathbf{s}(t)$ be two planar curves, regarded as complex functions of a real parameter $t \in [0, 1]$. We define

$$\text{distance}(\mathbf{r}, \mathbf{s}) = \sqrt{\|\mathbf{r}\|^2 + \|\mathbf{s}\|^2 - 2 \operatorname{Re}(\langle \mathbf{r}, \mathbf{s} \rangle)}.$$

Some elementary cases of distances are noted in the following lemma.

Lemma 1. Let $\mathbf{r}(t)$ and $\mathbf{s}(t)$ be planar curves. Then:

1. If $\mathbf{s}(t)$ is a translate of $\mathbf{r}(t)$ by the complex value \mathbf{d} , $\text{distance}(\mathbf{r}, \mathbf{s}) = |\mathbf{d}|$.
2. If $\mathbf{s}(t)$ is a rotation of $\mathbf{r}(t)$ by angle θ , $\text{distance}(\mathbf{r}, \mathbf{s}) = 2(1 - \cos \theta) \|\mathbf{r}\|$.
3. If $\mathbf{s}(t)$ is a scaling of $\mathbf{r}(t)$ by the factor c , $\text{distance}(\mathbf{r}, \mathbf{s}) = |1 - c| \|\mathbf{r}\|$.

Proof. The proof follows from Definitions 1–3 and some elementary computations with complex numbers. \square

In some contexts it may be desirable for $\text{distance}(\mathbf{r}, \mathbf{s})$ to reflect only the differences of *shape*, and discount considerations of position, orientation, and scaling. If $\mathbf{r}(0) = \mathbf{s}(0) = 0$, this can be achieved by a rotation/scaling transformation that makes the vectors $\mathbf{r}(1) - \mathbf{r}(0)$ and $\mathbf{s}(1) - \mathbf{s}(0)$ coincident.

The preceding ideas were briefly mentioned in the problem of constructing spatial C^2 closed loops with prescribed arc lengths using PH curves [16] — the solutions can be characterized in terms of two complex polynomials $\mathbf{u}(t), \mathbf{v}(t)$ satisfying $\|\mathbf{u}\| = \|\mathbf{v}\| = 1/\sqrt{2}$, $\langle \mathbf{u}, \mathbf{v} \rangle = 0$, and thus $\text{distance}(\mathbf{u}, \mathbf{v}) = 1$.

3. Orthogonal planar curves

Since $|\text{Re}(\langle \mathbf{u}, \mathbf{v} \rangle)| \leq \|\mathbf{u}\| \|\mathbf{v}\|$ from the Cauchy–Schwarz inequality, an angle $\theta \in [0, \pi]$ between \mathbf{u} and \mathbf{v} may be defined by

$$\cos \theta = \frac{\text{Re}(\langle \mathbf{u}, \mathbf{v} \rangle)}{\|\mathbf{u}\| \|\mathbf{v}\|},$$

and we thereby obtain the cosine rule

$$\text{distance}^2(\mathbf{u}, \mathbf{v}) = \|\mathbf{u}\|^2 + \|\mathbf{v}\|^2 - 2 \|\mathbf{u}\| \|\mathbf{v}\| \cos \theta.$$

Definition 4. Two complex polynomials \mathbf{u} and \mathbf{v} are *orthogonal* if $\cos \theta = 0$ — i.e., $\text{Re}(\langle \mathbf{u}, \mathbf{v} \rangle) = 0$. In this case we have $\text{distance}(\mathbf{u}, \mathbf{v}) = \sqrt{\|\mathbf{u}\|^2 + \|\mathbf{v}\|^2}$, and we write $\mathbf{u} \perp \mathbf{v}$.

Although the focus herein is on PH curves, the above principles apply to *any* planar curves represented as complex-valued polynomial functions of a real variable, an approach to the study of planar curves promoted by Zwikker [17]. If $\mathbf{r}(t)$ and $\mathbf{s}(t)$ are Bézier curves of degree m and n , with control points $\mathbf{p}_0, \dots, \mathbf{p}_m$ and $\mathbf{q}_0, \dots, \mathbf{q}_n$, the product $\mathbf{r}(t)\bar{\mathbf{s}}(t)$ can be expressed [18] as

$$\mathbf{r}(t)\bar{\mathbf{s}}(t) = \sum_{k=0}^{m+n} \mathbf{z}_k \binom{m+n}{k} (1-t)^{m+n-k} t^k,$$

with

$$\mathbf{z}_k = \sum_{j=\max(0, k-n)}^{\min(m, k)} \frac{\binom{m}{j} \binom{n}{k-j}}{\binom{m+n}{k}} \mathbf{p}_j \bar{\mathbf{q}}_{k-j}, \quad k = 0, \dots, m+n. \tag{3}$$

Since the definite integral of every Bernstein basis function of degree $m+n$ over $[0, 1]$ is simply $1/(m+n+1)$, the inner product of $\mathbf{r}(t)$ and $\mathbf{s}(t)$ is

$$\langle \mathbf{r}, \mathbf{s} \rangle = \frac{\mathbf{z}_0 + \dots + \mathbf{z}_{m+n}}{m+n+1}.$$

Thus, for given control points $\mathbf{p}_0, \dots, \mathbf{p}_m$ of $\mathbf{r}(t)$, the orthogonality condition $\text{Re}(\langle \mathbf{r}, \mathbf{s} \rangle) = 0$ amounts to a single linear constraint on the real and imaginary parts of the control points $\mathbf{q}_0, \dots, \mathbf{q}_n$ of $\mathbf{s}(t)$, so the dimension of the subspace of degree n curves $\mathbf{s}(t)$ that are orthogonal to $\mathbf{r}(t)$ is $2n+1$. To explore this subspace in more detail, we set

$$(r_x(t), r_y(t)) = (\text{Re}(\mathbf{r}(t)), \text{Im}(\mathbf{r}(t))), \quad (s_x(t), s_y(t)) = (\text{Re}(\mathbf{s}(t)), \text{Im}(\mathbf{s}(t))),$$

and define

$$\begin{aligned} d(t) &:= \text{Re}(\mathbf{r}(t)\bar{\mathbf{s}}(t)) = r_x(t)s_x(t) + r_y(t)s_y(t), \\ c(t) &:= \text{Im}(\mathbf{r}(t)\bar{\mathbf{s}}(t)) = s_x(t)r_y(t) - s_y(t)r_x(t). \end{aligned}$$

Regarding $\mathbf{r}(t), \mathbf{s}(t)$ as vector functions, $d(t)$ is their dot product and $c(t)$ is the component of the cross product orthogonal to the (x, y) plane. Moreover, $\text{Re}(\langle \mathbf{r}, \mathbf{s} \rangle)$ and $\text{Im}(\langle \mathbf{r}, \mathbf{s} \rangle)$ are the integrals of $d(t)$ and $c(t)$ over $t \in [0, 1]$.

To construct orthogonal curves, it is convenient to employ an orthonormal polynomial basis. We choose here the Legendre basis on $t \in [0, 1]$ which may be expressed in terms of the Bernstein basis [19] as

$$L_k(t) = \sqrt{2k+1} \sum_{i=0}^k (-1)^{k+i} \binom{k}{i} b_i^k(t), \quad b_i^k(t) = \binom{k}{i} (1-t)^{k-i} t^i.$$

These basis functions satisfy

$$\int_0^1 L_j(t)L_k(t) dt = \delta_{jk},$$

where δ_{jk} is the Kronecker delta, and the first few instances are

$$\begin{aligned} L_0(t) &= 1, \\ L_1(t) &= \sqrt{3}(2t - 1), \\ L_2(t) &= \sqrt{5}(6t^2 - 6t + 1), \\ L_3(t) &= \sqrt{7}(20t^3 - 30t^2 + 12t - 1). \end{aligned}$$

For any given curve $\mathbf{r}(t)$, $t \in [0, 1]$ of degree m we consider the problem of constructing curves $\mathbf{r}_\perp(t)$, of the same degree, that are orthogonal to $\mathbf{r}(t)$. The results are given in the following theorem.

Theorem 1. Let a given curve $\mathbf{r}(t)$ and a curve $\mathbf{r}_\perp(t)$ orthogonal to it be expressed in the Legendre basis as

$$\mathbf{r}(t) = \sum_{k=0}^m a_{k,1} L_k(t) + i \sum_{k=0}^m a_{k,2} L_k(t), \quad \mathbf{r}_\perp(t) = \sum_{k=0}^m b_{k,1} L_k(t) + i \sum_{k=0}^m b_{k,2} L_k(t), \tag{4}$$

and let

$$\mathbf{a} = (a_{0,1}, a_{0,2}, a_{1,1}, a_{1,2}, \dots, a_{m,1}, a_{m,2})^T \in \mathbb{R}^{2m+2}, \quad \mathbf{b} = (b_{0,1}, b_{0,2}, b_{1,1}, b_{1,2}, \dots, b_{m,1}, b_{m,2})^T \in \mathbb{R}^{2m+2} \tag{5}$$

be the vectors of the real and imaginary parts of their coefficients. Moreover, let

$$\mathbf{Q} = \mathbf{I} - \frac{2}{\mathbf{g}^T \mathbf{g}} \mathbf{g} \mathbf{g}^T, \quad \mathbf{g} = \mathbf{a} + \text{sign}(a_{0,1}) \|\mathbf{a}\|_2 \mathbf{e}_1, \quad \mathbf{e}_1 = (1, 0, \dots, 0)^T, \tag{6}$$

be a $(2m + 2) \times (2m + 2)$ orthogonal (Householder reflection) matrix, with columns \mathbf{q}_j , $j = 1, 2, \dots, 2m + 2$. Then any vector

$$\mathbf{b} = \sum_{k=2}^{2m+2} \xi_{k-1} \mathbf{q}_k, \quad \xi_1, \dots, \xi_{2m+1} \in \mathbb{R}, \tag{7}$$

identifies a curve $\mathbf{r}_\perp(t)$ of the form (4), that is orthogonal to $\mathbf{r}(t)$. Moreover, the columns of \mathbf{Q} also define curves that are pairwise orthogonal.

Proof. By the orthonormality of the Legendre basis polynomials, we have

$$\text{Re}(\langle \mathbf{r}, \mathbf{r}_\perp \rangle) = \int_0^1 \sum_{k=0}^m a_{k,1} L_k(t) \sum_{\ell=0}^m b_{\ell,1} L_\ell(t) + \sum_{k=0}^m a_{k,2} L_k(t) \sum_{\ell=0}^m b_{\ell,2} L_\ell(t) dt = \sum_{k=0}^m a_{k,1} b_{k,1} + a_{k,2} b_{k,2}.$$

Thus, identifying the coefficients $b_{k,1} + i b_{k,2}$, $k = 0, 1, \dots, m$, of an orthogonal curve is equivalent to finding the set of $2m + 1$ linearly independent vectors \mathbf{b} of the form (5) that are orthogonal to the vector \mathbf{a} with respect to the Euclidean inner (or dot) product in \mathbb{R}^{2m+2} . The basis of the orthogonal complement \mathbf{a}^\perp follows from the extended QR decomposition $\mathbf{a} = \mathbf{Q}\mathbf{R}$, where \mathbf{Q} is a $(2m + 2) \times (2m + 2)$ orthogonal matrix, defined by (6), and $\mathbf{R} = (\|\mathbf{a}\|_2, 0, \dots, 0)^T$. Here $\|\cdot\|_2$ is the standard Euclidean norm. Thus, any vector (7) identifies a curve $\mathbf{r}_\perp(t)$ of the form (4), that is orthogonal to $\mathbf{r}(t)$. Since the columns of \mathbf{Q} are pairwise orthogonal, the columns of \mathbf{Q} clearly also define curves that are pairwise orthogonal. \square

Example 1. Consider the vector $\mathbf{a} = (\alpha_0, 0, 0, \alpha_1, \alpha_2, 0, 0, \alpha_3)$ that defines the curve

$$\mathbf{r}(t) = \alpha_0 L_0(t) + \alpha_2 L_2(t) + i(\alpha_1 L_1(t) + \alpha_3 L_3(t)),$$

with Bézier control points

$$\mathbf{p}_0 = \alpha_0 + \sqrt{5} \alpha_2 - i(\sqrt{3} \alpha_1 + \sqrt{7} \alpha_3) = \bar{\mathbf{p}}_3,$$

$$\mathbf{p}_1 = \alpha_0 - \sqrt{5} \alpha_2 - i \left(\frac{\alpha_1}{\sqrt{3}} - 3\sqrt{7} \alpha_3 \right) = \bar{\mathbf{p}}_2.$$

In this case, we obtain

$$\mathbf{Q} = \begin{bmatrix} -\frac{\alpha_0}{\alpha} & 0 & 0 & -\frac{\alpha_1}{\alpha} & -\frac{\alpha_2}{\alpha} & 0 & 0 & -\frac{\alpha_3}{\alpha} \\ 0 & 1 & 0 & 0 & 0 & 0 & 0 & 0 \\ 0 & 0 & 1 & 0 & 0 & 0 & 0 & 0 \\ -\frac{\alpha_1}{\alpha} & 0 & 0 & 1 - \frac{\alpha_1^2}{\alpha^2 + \alpha_0 \alpha} & -\frac{\alpha_1 \alpha_2}{\alpha^2 + \alpha_0 \alpha} & 0 & 0 & -\frac{\alpha_1 \alpha_3}{\alpha^2 + \alpha_0 \alpha} \\ -\frac{\alpha_2}{\alpha} & 0 & 0 & -\frac{\alpha_1 \alpha_2}{\alpha^2 + \alpha_0 \alpha} & 1 - \frac{\alpha_2^2}{\alpha^2 + \alpha_0 \alpha} & 0 & 0 & -\frac{\alpha_2 \alpha_3}{\alpha^2 + \alpha_0 \alpha} \\ 0 & 0 & 0 & 0 & 0 & 1 & 0 & 0 \\ 0 & 0 & 0 & 0 & 0 & 0 & 1 & 0 \\ -\frac{\alpha_3}{\alpha} & 0 & 0 & -\frac{\alpha_1 \alpha_3}{\alpha^2 + \alpha_0 \alpha} & -\frac{\alpha_2 \alpha_3}{\alpha^2 + \alpha_0 \alpha} & 0 & 0 & 1 - \frac{\alpha_3^2}{\alpha^2 + \alpha_0 \alpha} \end{bmatrix},$$

where $\alpha = \|\mathbf{a}\|_2$. From columns 2, 3, 6, 7, we see that any curve of the form

$$\mathbf{r}_\perp(t) = \beta_1 L_1(t) + \beta_3 L_3(t) + i(\beta_0 L_0(t) + \beta_2 L_2(t)) \tag{8}$$

is orthogonal to $\mathbf{r}(t)$. The Bézier control points of such a curve are

$$\mathbf{q}_0 = -\sqrt{3}\beta_1 - \sqrt{7}\beta_3 + i(\beta_0 + \sqrt{5}\beta_2) = -\bar{\mathbf{q}}_3,$$

$$\mathbf{q}_1 = -\frac{\beta_1}{\sqrt{3}} + 3\sqrt{7}\beta_3 + i(\beta_0 - \sqrt{5}\beta_2) = -\bar{\mathbf{q}}_2.$$

Columns 4, 5, 8 of Q define three additional linearly-independent orthogonal curves, that are symmetric about the real axis. As an illustrative example, consider the case

$$\alpha_0 = 1, \alpha_1 = -2\sqrt{3}, \alpha_2 = \sqrt{5}, \alpha_3 = \sqrt{7}.$$

Fig. 1 shows the curve $\mathbf{r}(t)$ (black) and four curves $\mathbf{r}_\perp(t)$ orthogonal to it, corresponding to the columns 4 (red), 5 (green) and 8 (blue) of Q , multiplied by the norm of $\mathbf{r}(t)$, while the purple curve is defined by (8) with

$$\beta_0 = -1, \beta_1 = 3, \beta_2 = -2, \beta_3 = -4.$$

Fig. 1 also shows the graphs of $\text{Re}(\mathbf{r}(t)\mathbf{r}_\perp(t))$ for these four curves, which exhibit equal areas above and below the t -axis.

Example 2. The cubic curve

$$\mathbf{r}(t) = 7b_1^3(t) + \frac{16}{3}b_2^3(t) + i\left(\frac{20}{3}b_1^3(t) - \frac{11}{3}b_2^3(t) + \frac{19}{3}b_3^3(t)\right)$$

is a PH curve, since $\mathbf{r}'(t) = [5b_0^1(t) - 3b_1^1(t) + i(2b_0^1(t) - 5b_1^1(t))]^2$. From its Legendre coefficients, we obtain the vector

$$\mathbf{a} = \left(\frac{37}{12}, \frac{7}{3}, -\frac{\sqrt{3}}{12}, \frac{13\sqrt{3}}{30}, -\frac{37\sqrt{5}}{60}, \frac{\sqrt{5}}{6}, \frac{\sqrt{7}}{28}, \frac{4\sqrt{7}}{15}\right),$$

and columns 2–8 of its QR decomposition define 7 orthogonal curves $\mathbf{r}_{\perp,k}(t)$, $k = 1, \dots, 7$. We compute their linear combination

$$\mathbf{r}_\perp(t) = \sum_{k=1}^7 \xi_k \mathbf{r}_{\perp,k}(t),$$

so that $\mathbf{r}_\perp(t)$ is a PH curve. To equate the number of equations and unknowns ξ_1, \dots, ξ_7 we also require $\mathbf{r}_\perp(0) = 0$, and $\mathbf{r}_\perp(t)$ to have a prescribed parametric speed, $\sigma(t) = 20 - 40t + 38t^2$. The resulting non-linear system has six different solutions, illustrated in Fig. 2. Note that the prescribed $\sigma(t)$ implies that curves $\mathbf{r}(t)$ and $\mathbf{r}_\perp(t)$ all have the same arc length, namely $38/3$.

4. Planar Pythagorean-hodograph curves

Planar PH curves $\mathbf{r}(t)$ are generated from complex pre-image polynomials $\mathbf{w}(t)$ by integrating the derivative or *hodograph* $\mathbf{h}(t) := \mathbf{r}'(t) = \mathbf{w}^2(t)$. If $\mathbf{w}(t)$ is of degree m , specified in Bernstein form as

$$\mathbf{w}(t) = \sum_{k=0}^m \mathbf{w}_k b_k^m(t), \tag{9}$$

the hodograph may be written as

$$\mathbf{h}(t) = \sum_{k=0}^{2m} \mathbf{h}_k b_k^{2m}(t),$$

with coefficients determined [18] by using (3) as

$$\mathbf{h}_k = \sum_{j=\max(0,k-m)}^{\min(m,k)} \frac{\binom{m}{j} \binom{m}{k-j}}{\binom{2m}{k}} \mathbf{w}_j \mathbf{w}_{k-j}, \quad 0 \leq k \leq 2m. \tag{10}$$

The Bézier control points of the PH curve of degree $n = 2m + 1$ constructed by integrating $\mathbf{r}'(t)$ are then given by

$$\mathbf{p}_{k+1} = \mathbf{p}_k + \frac{\mathbf{h}_k}{2m+1}, \quad k = 0, \dots, n-1, \tag{11}$$

where we henceforth assume $\mathbf{p}_0 = 0$ as the integration constant.

We focus mainly on the planar PH quintics, generated from a quadratic pre-image polynomial (9), which are widely considered to be the lowest-order PH curves appropriate to free-form design applications. The control points of the Bézier form

$$\mathbf{r}(t) = \sum_{k=0}^5 \mathbf{p}_k b_k^5(t),$$

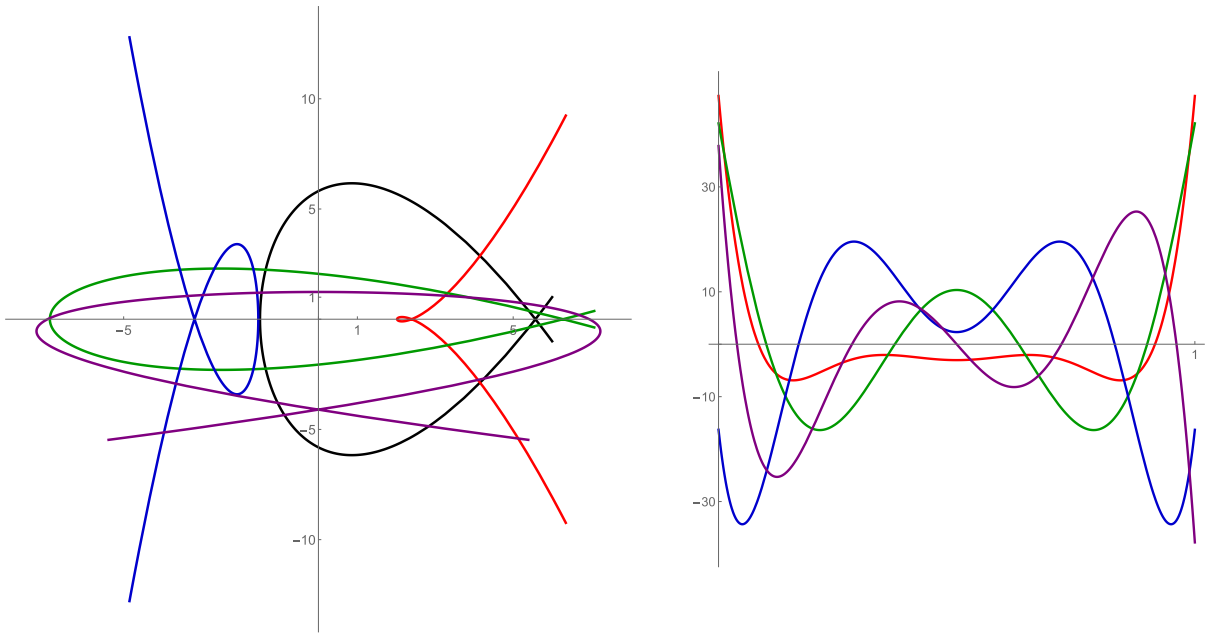


Fig. 1. Left: the curve $r(t)$ in Example 1 is indicated in black, and four curves $r_{\perp}(t)$ orthogonal to it are shown in red, green, blue, and purple. Right: the graphs of $\text{Re}(r(t)r_{\perp}(t))$ for these four curves.

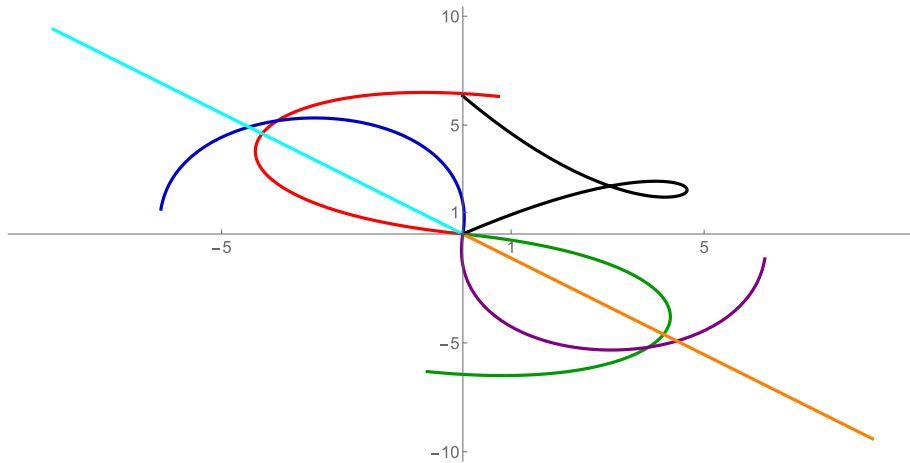


Fig. 2. The cubic PH curve $r(t)$ (black) in Example 2, together with the six PH curves $r_{\perp}(t)$ orthogonal to it (shown in different colors) that possess the same start point $(0,0)$ and have the prescribed parametric speed $\sigma(t)$.

are

$$\begin{aligned}
 \mathbf{p}_1 &= \mathbf{p}_0 + \frac{1}{5} \mathbf{w}_0^2, & \mathbf{p}_2 &= \mathbf{p}_1 + \frac{1}{5} \mathbf{w}_0 \mathbf{w}_1, \\
 \mathbf{p}_3 &= \mathbf{p}_2 + \frac{1}{5} \frac{2 \mathbf{w}_1^2 + \mathbf{w}_0 \mathbf{w}_2}{3}, \\
 \mathbf{p}_4 &= \mathbf{p}_3 + \frac{1}{5} \mathbf{w}_1 \mathbf{w}_2, & \mathbf{p}_5 &= \mathbf{p}_4 + \frac{1}{5} \mathbf{w}_2^2.
 \end{aligned}$$

Planar PH quintics are typically constructed as solutions to a first-order Hermite interpolation problem [20] for specified end points $\mathbf{r}(0), \mathbf{r}(1)$ and end derivatives $\mathbf{r}'(0), \mathbf{r}'(1)$. It is not feasible to modify their shape *a posteriori* by manipulating the control points, since this will ordinarily compromise their PH nature. Modifications that preserve the PH property of a curve should be made to its pre-image polynomial, rather than directly to the PH curve. The metric will, therefore, be primarily used to measure the distance between an original and modified pre-image polynomial of the PH curve it generates.

5. Perturbation of pre-image polynomials

A key application of the metric for complex polynomials is to provide a means to make “modest” shape changes to PH curves that preserve the PH property. To achieve this, modifications must be made to the pre-image polynomial. We consider perturbations $\delta\mathbf{w}(t)$ to a given pre-image polynomial $\mathbf{w}(t)$ that, for a prescribed bound Δ , satisfy

$$\text{distance}(\mathbf{w}, \mathbf{w} + \delta\mathbf{w}) = \|\delta\mathbf{w}\| \leq \Delta. \tag{12}$$

The perturbed pre-image polynomial determines a perturbed PH curve with control points \mathbf{p}_k displaced to $\mathbf{p}_k + \delta\mathbf{p}_k$ for $k = 1, \dots, n$. The perturbations $\delta\mathbf{p}_k$ may be obtained by replacing \mathbf{w}_k by $\mathbf{w}_k + \delta\mathbf{w}_k$ in (10) and (11), and they determine a perturbation $\delta\mathbf{r}(t)$, whose norm provides a measure of the difference between the modified and original curves.

Henceforth, we use the Legendre and Bernstein forms of both $\mathbf{w}(t)$ and $\delta\mathbf{w}(t)$ interchangeably. Whereas the former provides more concise formulations, the latter is the standard representation scheme in computer aided geometric design and offers simpler implementation of certain constraints, such as the preservation of initial/final tangent directions.

The following lemma [19] describes the transformation between these two representations, which is known to be numerically quite stable.

Lemma 2. For a polynomial $p(t)$ of degree n expressed in the Legendre and Bernstein bases on $[0, 1]$ as

$$p(t) = \sum_{k=0}^n c_k L_k(t) = \sum_{j=0}^n d_j b_j^n(t),$$

the coefficients $\mathbf{C} = (c_0, \dots, c_n)^T$ and $\mathbf{D} = (d_0, \dots, d_n)^T$ are related according to $\mathbf{D} = M_n \mathbf{C}$, where M_n is the $(n + 1) \times (n + 1)$ matrix with elements

$$M_{n,jk} = \frac{\sqrt{2k+1}}{\binom{n}{j}} \sum_{i=\max(0, j+k-n)}^{\min(j,k)} (-1)^{k+i} \binom{k}{i} \binom{k}{i} \binom{n-k}{j-i}, \quad 0 \leq j, k \leq n,$$

whose inverse M_n^{-1} has elements

$$M_{n,jk}^{-1} = \frac{\sqrt{2j+1}}{n+j+1} \binom{n}{k} \sum_{i=0}^j (-1)^{i+j} \frac{\binom{j}{i} \binom{j}{i}}{\binom{n+j}{k+i}}, \quad 0 \leq j, k \leq n.$$

Note that the columns of the matrix M_n are orthogonal, and the spectral norms are equal to

$$\|M_n\|_2 = \sigma_{\max}(M_n) = \sqrt{(2n+1) \binom{2n}{n}}, \quad \|M_n^{-1}\|_2 = \sigma_{\max}(M_n^{-1}) = \frac{1}{\sqrt{n+1}}. \tag{13}$$

Example 3. For the linear, quadratic, and cubic pre-image polynomials of cubic, quintic, and septic PH curves, the matrices M_n and their inverses are

$$M_1 = \begin{bmatrix} 1 & -\sqrt{3} \\ 1 & \sqrt{3} \end{bmatrix}, \quad M_1^{-1} = \begin{bmatrix} \frac{1}{2} & \frac{1}{2} \\ -\frac{\sqrt{3}}{6} & \frac{\sqrt{3}}{6} \end{bmatrix},$$

$$M_2 = \begin{bmatrix} 1 & -\sqrt{3} & \sqrt{5} \\ 1 & 0 & -2\sqrt{5} \\ 1 & \sqrt{3} & \sqrt{5} \end{bmatrix}, \quad M_2^{-1} = \begin{bmatrix} \frac{1}{3} & \frac{1}{3} & \frac{1}{3} \\ -\frac{\sqrt{3}}{6} & 0 & \frac{\sqrt{3}}{6} \\ \frac{\sqrt{5}}{30} & -\frac{\sqrt{5}}{15} & \frac{\sqrt{5}}{30} \end{bmatrix},$$

$$M_3 = \begin{bmatrix} 1 & -\sqrt{3} & \sqrt{5} & -\sqrt{7} \\ 1 & -\frac{\sqrt{3}}{3} & -\sqrt{5} & 3\sqrt{7} \\ 1 & \frac{\sqrt{3}}{3} & -\sqrt{5} & -3\sqrt{7} \\ 1 & \sqrt{3} & \sqrt{5} & \sqrt{7} \end{bmatrix}, \quad M_3^{-1} = \begin{bmatrix} \frac{1}{4} & \frac{1}{4} & \frac{1}{4} & \frac{1}{4} \\ -\frac{3\sqrt{3}}{20} & -\frac{\sqrt{3}}{20} & \frac{\sqrt{3}}{20} & \frac{3\sqrt{3}}{20} \\ \frac{\sqrt{5}}{20} & -\frac{\sqrt{5}}{20} & -\frac{\sqrt{5}}{20} & \frac{\sqrt{5}}{20} \\ -\frac{\sqrt{7}}{140} & \frac{\sqrt{7}}{140} & -\frac{3\sqrt{7}}{140} & \frac{\sqrt{7}}{140} \end{bmatrix}.$$

In the Legendre form, the pre-image polynomial (9) is expressed in terms of coefficients $\mathbf{c}_0, \dots, \mathbf{c}_m$ as

$$\mathbf{w}(t) = \sum_{k=0}^m \mathbf{c}_k L_k(t), \tag{14}$$

and the Bernstein coefficients can be recovered from the Legendre coefficients through the relations

$$\mathbf{w}_j = \sum_{k=0}^m M_{m,jk} \mathbf{c}_k, \quad j = 0, \dots, m, \tag{15}$$

from which the Bézier control points (11) may be determined. The Legendre and Bernstein forms of the perturbation polynomial are

$$\delta w(t) = \sum_{k=0}^m \delta c_k L_k(t) = \sum_{j=0}^m \delta w_j b_j^m(t). \tag{16}$$

The relations (15) also hold for δw_j in terms of δc_k , i.e.,

$$\delta W = M_m \delta C, \quad \delta W := (\delta w_0, \dots, \delta w_m)^T, \quad \delta C := (\delta c_0, \dots, \delta c_m)^T. \tag{17}$$

In the Legendre form, the norm of the perturbation $\delta w(t)$ is clearly equal to

$$\|\delta w\| = \sqrt{|\delta c_0|^2 + \dots + |\delta c_m|^2} = \|\delta C\|_2, \tag{18}$$

where $\|\cdot\|_2$ again denotes the standard Euclidean norm. The next lemma follows directly from this equality.

Lemma 3. Writing the perturbation coefficients of (16) in the Legendre form as

$$\delta c_k = \rho_k \exp(i \varphi_k), \quad k = 0, \dots, m, \tag{19}$$

the inequality (12), i.e., $\|\delta w\| \leq \Delta$, is for any given Δ satisfied if and only if

$$\sqrt{\sum_{k=0}^m \rho_k^2} \leq \Delta.$$

For perturbations of equal magnitude $\rho := \rho_0 = \dots = \rho_m$ the inequality (12) is fulfilled iff $\rho \leq \Delta / \sqrt{m + 1}$.

The next lemma reveals simple sufficient conditions to satisfy (12) in the case of the Bernstein representation.

Lemma 4. Let the coefficients of δw in the Bernstein form be expressed as

$$\delta w_k = r_k \exp(i \phi_k), \quad k = 0, \dots, m. \tag{20}$$

If

$$\sqrt{\sum_{k=0}^m r_k^2} \leq \sqrt{m + 1} \Delta$$

for a given Δ , then the inequality (12), i.e., $\|\delta w\| \leq \Delta$, is satisfied. In the case of equal-magnitude perturbations, $r := r_0 = \dots = r_m$, the simple choice $r \leq \Delta$ implies that (12) holds true.

Proof. In the Bernstein form $\|\delta w\|$ may be expressed, using (17) and (18), as

$$\|\delta w\| = \|M_m^{-1} \delta W\|_2.$$

Since

$$\|M_m^{-1} \delta W\|_2 \leq \|M_m^{-1}\|_2 \|\delta W\|_2,$$

where $\|M_m^{-1}\|_2$ is the matrix norm induced by the Euclidean vector norm (spectral norm), which is equal to the largest singular value $\sigma_{\max}(M_m^{-1}) = 1/\sqrt{m + 1}$ (see (13)), any choice of coefficients δW such that $\|\delta W\|_2 \leq \sqrt{m + 1} \Delta$ ensures (12) for any given Δ . The equality $\|\delta W\|_2 = \sqrt{\sum_{k=0}^m r_k^2}$ completes the proof. \square

The Legendre representation allows us to express in a simple way the sufficient and necessary condition for (12) to hold true. On the other hand, for the Bernstein representation, Lemma 4 provides a simple sufficient condition, but to express a necessary condition is much more complicated, as shown in the next remark, which reveals strict bounds in the case of equal-magnitude perturbations for low degree cases.

Remark 1. Let the coefficients of δw in the Bernstein form be expressed by (20) with $r := r_0 = \dots = r_m$. The inequality (12) is satisfied if and only if

$$\begin{aligned} \|\delta w\| &= \frac{\sqrt{\Phi_{01} + 2}}{\sqrt{3}} r \leq \Delta, \\ \|\delta w\| &= \frac{\sqrt{3\Phi_{01} + \Phi_{02} + 3\Phi_{12} + 8}}{\sqrt{15}} r \leq \Delta, \\ \|\delta w\| &= \frac{\sqrt{10\Phi_{01} + 4\Phi_{02} + \Phi_{03} + 9\Phi_{12} + 4\Phi_{13} + 10\Phi_{23} + 32}}{\sqrt{70}} r \leq \Delta, \end{aligned} \tag{21}$$

for $m = 1, 2, 3$, respectively, which follow from straightforward computations using the matrices in Example 3 and the notation $\Phi_{ij} := \cos(\phi_i - \phi_j)$. In each case, the factors multiplying r in (21) are bounded from above by 1.

From Eq. (18), we see that the Euclidean norm of Legendre perturbation coefficients is equal to the norm of the perturbation. However, for the Bernstein coefficients, we only have an upper bound

$$\|\delta \mathbf{W}\|_2 = \|M_m \delta \mathbf{C}\|_2 \leq \|M_m\|_2 \|\delta \mathbf{C}\|_2 = \sqrt{(2m+1) \binom{2m}{m}} \|\delta \mathbf{w}\|. \tag{22}$$

Note that usually (see, e.g., Lemma 4) the norm $\|\delta \mathbf{W}\|_2$ is much lower than this bound.

It remains to analyze the distance between the original and the modified PH curve in terms of the bound (12) on the pre-image perturbation. Let the original pre-image $\mathbf{w}(t)$ be given by (9) and let the perturbation (16) be such that $\|\delta \mathbf{w}\| \leq \Delta$ for some chosen Δ . The difference between the modified PH curve

$$\tilde{\mathbf{r}}(t) = \int_0^t (\mathbf{w}(\tau) + \delta \mathbf{w}(\tau))^2 d\tau + \tilde{\mathbf{p}}_0$$

and the original PH curve is

$$\delta \mathbf{r}(t) = \tilde{\mathbf{r}}(t) - \mathbf{r}(t) = \int_0^t \delta \mathbf{h}(\tau) d\tau + \delta \mathbf{p}_0, \quad \delta \mathbf{h}(t) := 2\mathbf{w}(t)\delta \mathbf{w}(t) + \delta \mathbf{w}(t)^2, \quad \delta \mathbf{p}_0 := \tilde{\mathbf{p}}_0 - \mathbf{p}_0, \tag{23}$$

where $\delta \mathbf{p}_0$ depends on the choice of the integration constant and not on the perturbation in the pre-image space. The next theorem provides a simple upper bound for the norm of $\delta \mathbf{r}(t)$.

Theorem 2. *The distance between the original and the modified PH curve can be bounded from above by*

$$\|\delta \mathbf{r}\| \leq |\delta \mathbf{p}_0| + 2 \|\mathbf{W}\|_\infty \|\delta \mathbf{W}\|_\infty + \|\delta \mathbf{W}\|_\infty^2,$$

where $\mathbf{W} = (\mathbf{w}_0, \dots, \mathbf{w}_m)^T$ and $\delta \mathbf{W} = (\delta \mathbf{w}_0, \dots, \delta \mathbf{w}_m)^T$ are vectors of Bernstein coefficients of $\mathbf{w}(t)$ and $\delta \mathbf{w}(t)$, given by (9) and (16), and

$$\|\mathbf{W}\|_\infty = \max_{j=0, \dots, m} |\mathbf{w}_j|, \quad \|\delta \mathbf{W}\|_\infty = \max_{j=0, \dots, m} |\delta \mathbf{w}_j|$$

are the infinity vector norms.

Proof. We use the notation

$$\delta \mathbf{r}(t) = \sum_{k=0}^{2m+1} \delta \mathbf{p}_k b_k^{2m+1}(t), \quad \delta \mathbf{P} := (\delta \mathbf{p}_0, \dots, \delta \mathbf{p}_{2m+1})^T, \quad \delta \mathbf{h}(t) = \sum_{k=0}^{2m} \delta \mathbf{h}_k b_k^{2m}(t), \quad \delta \mathbf{H} := (\delta \mathbf{h}_0, \dots, \delta \mathbf{h}_{2m})^T,$$

where the Bernstein coefficients are by (23) related as

$$\delta \mathbf{p}_k = \delta \mathbf{p}_0 + \frac{1}{2m+1} \sum_{j=0}^{k-1} \delta \mathbf{h}_j, \quad k = 1, 2, \dots, 2m+1.$$

With the same arguments as in the proof of Lemma 4, we obtain

$$\|\delta \mathbf{r}\| = \left\| M_{2m+1}^{-1} \delta \mathbf{P} \right\|_2 \leq \left\| M_{2m+1}^{-1} \right\|_2 \|\delta \mathbf{P}\|_2 = \frac{1}{\sqrt{2m+2}} \|\delta \mathbf{P}\|_2 \leq \max_{k=0, \dots, 2m+1} |\delta \mathbf{p}_k| = \|\delta \mathbf{P}\|_\infty.$$

So the distance between the original and modified PH curves can be bounded from above by the infinity vector norm of $\delta \mathbf{P}$. Since

$$|\delta \mathbf{p}_k| \leq |\delta \mathbf{p}_0| + \frac{1}{2m+1} \sum_{j=0}^{k-1} |\delta \mathbf{h}_j| \leq |\delta \mathbf{p}_0| + \frac{1}{2m+1} \sum_{j=0}^{2m} |\delta \mathbf{h}_j| \leq |\delta \mathbf{p}_0| + \max_{j=0, \dots, 2m} |\delta \mathbf{h}_j|$$

for any k , we have $\|\delta \mathbf{P}\|_\infty \leq |\delta \mathbf{p}_0| + \|\delta \mathbf{H}\|_\infty$. Applying the formula (3), we see that the Bernstein coefficients of $\delta \mathbf{h}(t) = 2\mathbf{w}(t)\delta \mathbf{w}(t) + \delta \mathbf{w}(t)^2$ are equal to

$$\delta \mathbf{h}_k = \sum_{j=\max(0, k-m)}^{\min(m, k)} \frac{\binom{m}{j} \binom{m}{k-j}}{\binom{2m}{k}} (2\mathbf{w}_j \delta \mathbf{w}_{k-j} + \delta \mathbf{w}_j \delta \mathbf{w}_{k-j}), \quad k = 0, \dots, 2m.$$

Moreover, applying (3) for constant polynomials and the partition of unity property gives

$$\sum_{j=\max(0, k-m)}^{\min(m, k)} \frac{\binom{m}{j} \binom{m}{k-j}}{\binom{2m}{k}} = 1 \quad \text{for all } k = 0, \dots, 2m,$$

which directly implies that

$$|\delta \mathbf{h}_k| \leq 2 \max_{j=0, \dots, m} |\mathbf{w}_j| \max_{j=0, \dots, m} |\delta \mathbf{w}_j| + \left(\max_{j=0, \dots, m} |\delta \mathbf{w}_j| \right)^2$$

for any $k = 0, 1, \dots, 2m$, and the proof is complete. \square

Corollary 1. Suppose that $\|\delta\mathbf{w}\| \leq \Delta$, and choose the integration constant so that $\delta\mathbf{p}_0 = 0$. Since $\|\delta\mathbf{W}\|_\infty \leq \|\delta\mathbf{W}\|_2$ we obtain

$$\|\delta\mathbf{r}\| \leq 2 c(m) \Delta \|\mathbf{W}\|_\infty + (c(m) \Delta)^2,$$

where $c(m)$ is a constant, that depends only on the degree m , and can by (22) be taken as $c(m) = \sqrt{(2m + 1)\binom{2m}{m}}$. Under the assumptions of Lemma 4 we can lower the upper bound by taking $c(m) = \sqrt{m + 1}$, or $c(m) = 1$ in the case of equal-magnitude perturbations.

Although the upper bound in Corollary 1 may be much higher than the value of the distance $\|\delta\mathbf{r}\|$, it shows that the distance between the original and the modified PH curve goes to zero when Δ goes to zero, provided that $|\delta\mathbf{p}_0|$ is zero or also converges to zero.

5.1. Preservation of curve end tangent directions

Although the Bernstein form is more involved in terms of strictly satisfying the bound $\|\delta\mathbf{w}\| = \Delta$, it provides a simple means to preserve the directions of the curve end derivatives $\mathbf{r}'(0) = \mathbf{w}_0^2$ and $\mathbf{r}'(1) = \mathbf{w}_m^2$ by, for example, choosing $\phi_0 = \arg(\mathbf{w}_0)$ and $\phi_m = \arg(\mathbf{w}_m)$, leaving $\phi_1, \dots, \phi_{m-1}$ and r_0, \dots, r_m as free parameters — subject to (12) and (20) — to manipulate the curve shape. On the other hand, with the Legendre form and the perturbations (19), the equality $\|\delta\mathbf{w}\| = \Delta$ can be simply satisfied by, e.g., choosing $\rho_0 = \dots = \rho_m = \Delta/\sqrt{m + 1}$, but the analogous method for preserving the end derivative directions incurs the complicated conditions

$$\arg(\mathbf{w}_0) = \arg \left[\sum_{k=0}^m M_{m,0k} e^{i\phi_k} \right], \quad \arg(\mathbf{w}_m) = \arg \left[\sum_{k=0}^m M_{m,mk} e^{i\phi_k} \right]. \tag{24}$$

The following example illustrates these considerations.

Example 4. Consider the quadratic pre-image polynomial $\mathbf{w}(t)$ specified by Bernstein coefficients

$$\mathbf{w}_0 = 5 + 2i, \quad \mathbf{w}_1 = -3 - 4i, \quad \mathbf{w}_2 = 5 + i,$$

with corresponding Legendre coefficients

$$\mathbf{c}_0 = \frac{7}{3} - \frac{1}{3}i, \quad \mathbf{c}_1 = -\frac{\sqrt{3}}{6}i, \quad \mathbf{c}_2 = \frac{8\sqrt{5}}{15} + \frac{11\sqrt{5}}{30}i,$$

on which we impose perturbations of the form (19) and (20) for $m = 2$ with equal magnitudes $r = r_0 = r_1 = r_2$ and $\rho = \rho_0 = \rho_1 = \rho_2$, satisfying (12) with equality and $\Delta = 0.25$. With the Bézier representation, the end tangent directions are preserved by choosing $\phi_0 = \arg(\mathbf{w}_0) = \arctan(2/5)$ and $\phi_2 = \arctan(1/5)$. For $\phi_1 = 0, \pi/4, \pi/2, 3\pi/4$ we obtain from (21) the r values for which $\|\delta\mathbf{w}\| = 0.25$ as $r = 0.25245, 0.25661, 0.29620, 0.39083$, respectively. Fig. 3 depicts the original and four modified PH quintics, all satisfying $\|\delta\mathbf{w}\| = 0.25$ — their distances from the original PH quintic are 0.29691, 0.30096, 0.29884, 0.28626, respectively. Also shown is the envelope of the family of all possible perturbed curves with the prescribed end tangents, for $r = 0.25$. Note that all the curves have been shifted so that the centroids of their Bézier control points are coincident.

With the Legendre representation, the bound $\|\delta\mathbf{w}\| = 0.25$ is attained, for any angles ϕ_0, ϕ_1, ϕ_2 , if and only if $\rho = 0.25/\sqrt{3}$. To also preserve the end tangent directions, these angles must be chosen (see (24)) so as to satisfy

$$\begin{aligned} \arg(e^{i\phi_0} - \sqrt{3}e^{i\phi_1} + \sqrt{5}e^{i\phi_2}) &= \arctan(2/5), \\ \arg(e^{i\phi_0} + \sqrt{3}e^{i\phi_1} + \sqrt{5}e^{i\phi_2}) &= \arctan(1/5). \end{aligned}$$

For each of the values $\phi_0 = 0, \pi/4, \pi/2, 3\pi/4$, four distinct (ϕ_1, ϕ_2) solutions were identified, defining four different perturbations of the quintic PH curve. Fig. 4 compares the original PH curve with a representative perturbed PH quintic from each of the sets of four solutions. The modified PH quintics have distances 0.19350, 0.22553, 0.23572, 0.22451 from the original PH curve. The envelope of the family of modified curves for all ϕ_0 values and all solutions is also shown (all the curves are shifted so the centroids of their Bézier control points are coincident).

In the preceding discussion, the perturbations incur a global change in the curve. In particular, the curve end points change, which may be undesirable in common design contexts. Perturbations to the pre-image polynomials that preserve the curve endpoints are addressed next.

5.2. Preservation of curve end points

To eliminate non-essential freedoms, it is customary to consider construction of PH curves in canonical form [12,21] such that $\mathbf{r}(0) = 0$ and $\mathbf{r}(1) = 1$. The mapping of a PH curve with prescribed end points to and from canonical form can be achieved using a simple translation/rotation/scaling transformation. Thus, we confine our attention to canonical-form PH curves in investigating perturbations that preserve the curve end points. Taking $\mathbf{r}(0) = 0$ by choice of the integration constant, $\mathbf{r}(1) = 1$ is achieved through the condition

$$\int_0^1 \mathbf{r}'(t) dt = \int_0^1 \mathbf{w}^2(t) dt = \mathbf{r}(1) - \mathbf{r}(0) = 1. \tag{25}$$



Fig. 3. Left: The prescribed quintic PH curve (blue), with four instances modified using the Bernstein basis (different colors), whose pre-images satisfy $\|\delta\mathbf{w}\| = 0.25$, as described in Example 4. Right: The envelope of the family of all perturbed curves with preserved end tangent directions for $r = 0.25$.

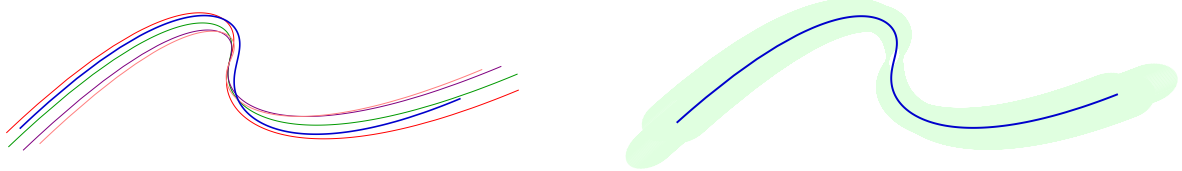


Fig. 4. Left: The prescribed quintic PH curve (blue) with four instances modified using the Legendre basis (different colors), whose pre-images satisfy $\|\delta\mathbf{w}\| = 0.25$, as described in Example 4. Right: The envelope of the family of all perturbed curves with preserved end tangent directions for $\rho = 0.25/\sqrt{3}$.

In the Bernstein and Legendre representations (9) and (14) of the pre-image polynomial $\mathbf{w}(t)$, we set $\mathbf{C} = (\mathbf{c}_0, \dots, \mathbf{c}_m)^T$ and $\mathbf{W} = (\mathbf{w}_0, \dots, \mathbf{w}_m)^T$. As in (17), the connection between these coefficients is defined by $\mathbf{W} = M_m \mathbf{C}$ (see Lemma 2). It is easy to see that, for the Legendre form (14), the constraint (25) reduces to

$$\mathbf{C}^T \mathbf{C} = \sum_{k=0}^m \mathbf{c}_k^2 = 1, \tag{26}$$

i.e., the Legendre coefficients correspond to points on the unit sphere in \mathbb{C}^{m+1} . Setting $\mathbf{C} = \mathbf{C}_R + i \mathbf{C}_I$, where $\mathbf{C}_R, \mathbf{C}_I \in \mathbb{R}^{m+1}$, we note that Eq. (26) is satisfied if and only if

$$\|\mathbf{C}_R\|_2^2 - \|\mathbf{C}_I\|_2^2 = 1 \quad \text{and} \quad \mathbf{C}_R^T \mathbf{C}_I = 0.$$

From $\mathbf{C} = M_m^{-1} \mathbf{W}$, the constraint (25) expressed in terms of the Bernstein coefficients becomes

$$\sum_{k=0}^m \mathbf{c}_k^2 = \mathbf{C}^T \mathbf{C} = (M_m^{-1} \mathbf{W})^T (M_m^{-1} \mathbf{W}) = \mathbf{W}^T (M_m^{-1})^T M_m^{-1} \mathbf{W} = 1. \tag{27}$$

Setting $G_m = (M_m^{-1})^T M_m^{-1}$, we obtain for $m = 1, 2, 3$ the $(m + 1) \times (m + 1)$ matrices with elements $g_{m,jk}$ for $0 \leq j, k \leq m$ as

$$G_1 = \frac{1}{6} \begin{bmatrix} 2 & 1 \\ 1 & 2 \end{bmatrix}, \quad G_2 = \frac{1}{30} \begin{bmatrix} 6 & 3 & 1 \\ 3 & 4 & 3 \\ 1 & 3 & 6 \end{bmatrix}, \quad G_3 = \frac{1}{140} \begin{bmatrix} 20 & 10 & 4 & 1 \\ 10 & 12 & 9 & 4 \\ 4 & 9 & 12 & 10 \\ 1 & 4 & 10 & 20 \end{bmatrix},$$

and in the cases $m = 1, 2, 3$ Eq. (27) then reduces to

$$\begin{aligned} \mathbf{w}_0^2 + \mathbf{w}_1^2 + \mathbf{w}_1 \mathbf{w}_0 &= 3, \\ 3 \mathbf{w}_0^2 + 3 \mathbf{w}_2^2 + 2 \mathbf{w}_1^2 + 3(\mathbf{w}_0 + \mathbf{w}_2) \mathbf{w}_1 + \mathbf{w}_0 \mathbf{w}_2 &= 15, \\ 10(\mathbf{w}_0^2 + \mathbf{w}_3^2) + 6(\mathbf{w}_1^2 + \mathbf{w}_2^2) + 10(\mathbf{w}_0 \mathbf{w}_1 + \mathbf{w}_2 \mathbf{w}_3) + 4(\mathbf{w}_2 \mathbf{w}_0 + \mathbf{w}_1 \mathbf{w}_3) + \mathbf{w}_3 \mathbf{w}_0 + 9 \mathbf{w}_1 \mathbf{w}_2 &= 70. \end{aligned}$$

To ensure that the conditions (26) and (27) are fulfilled upon substituting $\mathbf{c}_k \rightarrow \mathbf{c}_k + \delta\mathbf{c}_k$ and $\mathbf{w}_k \rightarrow \mathbf{w}_k + \delta\mathbf{w}_k$ for $k = 0, \dots, m$, the coefficients $\delta\mathbf{c}_k$ and $\delta\mathbf{w}_k$ must satisfy

$$\sum_{k=0}^m \delta\mathbf{c}_k^2 + 2 \sum_{k=0}^m \mathbf{c}_k \delta\mathbf{c}_k = \delta\mathbf{C}^T (\delta\mathbf{C} + 2\mathbf{C}) = 0, \tag{28}$$

and

$$\delta\mathbf{W}^T G_m (\delta\mathbf{W} + 2\mathbf{W}) = \sum_{j=0}^m \sum_{k=0}^m g_{m,jk} \delta\mathbf{w}_j (\delta\mathbf{w}_k + 2\mathbf{w}_k) = 0, \tag{29}$$

for the prescribed \mathbf{c}_k and \mathbf{w}_k values satisfying (26) and (27). In addition, the perturbations must satisfy the bounds $\|\delta\mathbf{C}\|_2 \leq \Delta$ and $\|M_m^{-1} \delta\mathbf{W}\|_2 \leq \Delta$. Writing $\delta\mathbf{C} = \delta\mathbf{C}_R + i \delta\mathbf{C}_I$, the condition (28) is equivalent to two scalar equations in the real vectors $\delta\mathbf{C}_R$ and $\delta\mathbf{C}_I$, namely

$$\begin{aligned} \|\delta\mathbf{C}_R\|_2^2 - \|\delta\mathbf{C}_I\|_2^2 + 2\delta\mathbf{C}_R^T \mathbf{C}_R - 2\delta\mathbf{C}_I^T \mathbf{C}_I &= 0, \\ \delta\mathbf{C}_R^T \delta\mathbf{C}_I + \delta\mathbf{C}_R^T \mathbf{C}_I + \delta\mathbf{C}_I^T \mathbf{C}_R &= 0. \end{aligned} \tag{30}$$

Writing $\delta\mathbf{W} = \delta\mathbf{W}_R + i\delta\mathbf{W}_I$, we have $\delta\mathbf{W}_R = M_m\delta\mathbf{C}_R$ and $\delta\mathbf{W}_I = M_m\delta\mathbf{C}_I$, so these equations can also be expressed in terms of $\delta\mathbf{W}_R$ and $\delta\mathbf{W}_I$.

In general, the identification of perturbations $\delta\mathbf{w}$ that maintain the perturbed curve in canonical form and satisfy $\|\delta\mathbf{w}\| = d \leq \Delta$ for some chosen d entails the solution of a rather complicated non-linear system. The next lemma proposes a simple sufficient way to determine such perturbations.

Lemma 5. Suppose that $\mathbf{w}(t)$ of degree $m \geq 2$ is expressed in the Legendre basis (14) and induces the PH curve in canonical form. Further, assume that $\delta\mathbf{w}(t)$ is given by (16) with Legendre coefficients (19) for which the angles are all the same, i.e., $\varphi := \varphi_0 = \dots = \varphi_m$. Then $\|\delta\mathbf{w}\| = d$ for some chosen d , and the modified PH curve is in canonical form for any angle φ if and only if the radii ρ_k , $k = 0, 1, \dots, m$, satisfy one quadratic and two linear equations:

$$\sum_{k=0}^m \rho_k^2 = d^2, \tag{31}$$

and

$$\begin{aligned} d^2 \cos(2\varphi) + 2 \sum_{k=0}^m \rho_k (\cos(\varphi) \operatorname{Re}(\mathbf{c}_k) - \sin(\varphi) \operatorname{Im}(\mathbf{c}_k)) &= 0, \\ d^2 \sin(2\varphi) + 2 \sum_{k=0}^m \rho_k (\cos(\varphi) \operatorname{Im}(\mathbf{c}_k) + \sin(\varphi) \operatorname{Re}(\mathbf{c}_k)) &= 0. \end{aligned} \tag{32}$$

Proof. The quadratic equation follows directly from (18) and (19). Using the assumption $\varphi = \varphi_0 = \dots = \varphi_m$ it is straightforward to compute that

$$\|\delta\mathbf{C}_R\|_2^2 - \|\delta\mathbf{C}_I\|_2^2 = \sum_{k=0}^m \rho_k^2 \cos(2\varphi), \quad \delta\mathbf{C}_R^T \delta\mathbf{C}_I = \frac{1}{2} \sum_{k=0}^m \rho_k^2 \sin(2\varphi).$$

Eqs. (32) follow then directly from (30) which are sufficient and necessary to obtain the canonical form of the modified PH curve. \square

The following example demonstrates the construction given in Lemma 5.

Example 5. Consider the quadratic pre-image polynomial with Legendre coefficients

$$\mathbf{c}_0 = 2 - i, \quad \mathbf{c}_1 = 1 + 2i, \quad \mathbf{c}_2 = -1 + 0i,$$

satisfying (26). We choose $d = 0.1$ for perturbations of the form (19) with $\varphi_0 = \dots = \varphi_m = \varphi$ for any $\varphi \in (-\pi, \pi]$. From (32) we obtain

$$\rho_1 = \frac{\rho_0}{2} - \frac{\sin(\varphi)}{400}, \quad \rho_2 = \frac{5\rho_0}{2} - \frac{\sin(\varphi)}{400} + \frac{\cos(\varphi)}{200},$$

and (31) reduces to a quadratic equation for ρ_0 , namely

$$\frac{15}{2} \rho_0^2 + \frac{5 \cos(\varphi) - 3 \sin(\varphi)}{200} \rho_0 + \frac{\cos(2\varphi) - 2 \sin(2\varphi) - 1597}{160000} = 0,$$

which has a positive discriminant for any φ . Thus, there are always two admissible perturbations $\delta\mathbf{w}$. For $\varphi = 0$ they are shown in Fig. 5 (left, red and green curves), together with the original (blue) curve, and the envelope of all solutions for $\varphi \in (-\pi, \pi]$.

With the Legendre representation, it is easy to construct perturbations $\delta\mathbf{w}(t)$ that preserve endpoints of the given curve, while the Bézier representation is more convenient for preserving end tangent directions. The constraints on the coefficients of $\delta\mathbf{w}(t)$ imposed by preserving endpoints and end tangent directions, coupled with the non-linear dependence of $\|\delta\mathbf{w}\|$ on those coefficients, make it difficult to formulate schemes that guarantee an *a priori* satisfaction of the bound (12). As a practical solution for PH quintics, we consider here coefficients $\delta\mathbf{w}_0 = r \exp(i\phi_0)$ and $\delta\mathbf{w}_2 = r \exp(i\phi_2)$, where $\phi_0 = \arg(\mathbf{w}_0)$ and $\phi_2 = \arg(\mathbf{w}_2)$, for a prescribed r value, to preserve the end tangent directions. Preservation of the endpoints can then be achieved by solving the $m = 2$ instance of Eq. (29) for $\mathbf{w}_0, \mathbf{w}_1, \mathbf{w}_2$ values that define a canonical-form PH quintic, as a quadratic equation in $\delta\mathbf{w}_1$. Since this incurs modest computational effort, it is amenable to real-time user modification of r to ensure satisfaction of (12). However, adding the constraint $\|\delta\mathbf{w}\| = d$ for some $d \leq \Delta$ adds one non-linear equation, but since the whole non-linear system is algebraic, it is possible to compute all the solutions using a computer algebra system.

Example 6. Consider a canonical-form PH quintic defined by a quadratic pre-image polynomial with Bernstein coefficients

$$\begin{aligned} \mathbf{w}_0 = \mathbf{w}_2 &= \sqrt{2} + \frac{\sqrt{2}}{2}i, \\ \mathbf{w}_1 &= \frac{\sqrt{5(9 + \sqrt{97})} - 6\sqrt{2}}{4} - \frac{\sqrt{-27 + 5\sqrt{97} + 6\sqrt{10(\sqrt{97} - 9)}}}{4}i. \end{aligned}$$

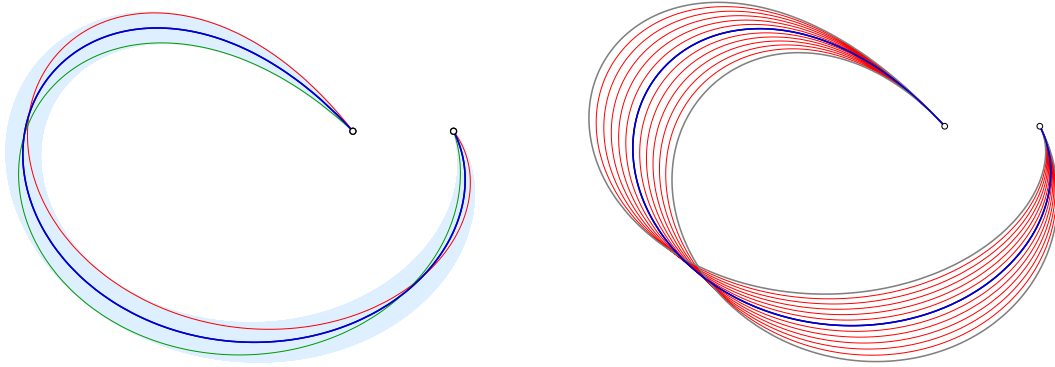


Fig. 5. Left: The perturbed PH quintics (red and green) for $\|\delta\mathbf{w}\| = 0.1$, with the same end points as the quintic PH curve (blue) in Example 5, defined by $\varphi = 0$. The envelope of all the solutions for $\varphi \in (-\pi, \pi]$ is also shown (light blue). Right: The modified PH quintic curves that preserve end points and end tangent directions, as described in Example 6, as $\|\delta\mathbf{w}\|$ varies.

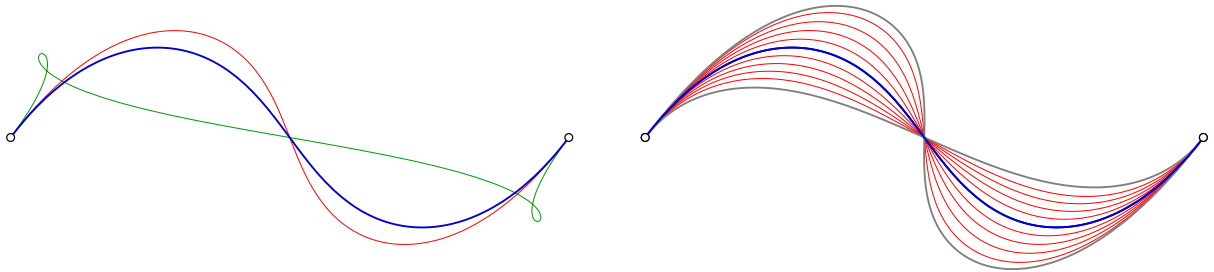


Fig. 6. Left: The given canonical-form PH quintic (blue) with two modifications (red, green) that preserve the endpoints and tangent directions for a fixed $r = 0.2$, as described in Example 6. Right: The modified curves satisfying $\|\delta\mathbf{w}\| \leq 0.25$ as r varies.

To preserve the end tangent angles $\theta_0 = \arg(\mathbf{w}_0)$ and $\theta_2 = \arg(\mathbf{w}_2)$, we set $\delta\mathbf{w}_0 = r \exp(i\theta_0)$, $\delta\mathbf{w}_2 = r \exp(i\theta_2)$ for some chosen r , and compute $\delta\mathbf{w}_1$ from Eq. (29) for $m = 2$. With $r = 0.2$ we obtain two solutions

$$\delta\mathbf{w}_1 = -0.33476348 - 0.29109547i, \quad \delta\mathbf{w}_1 = -5.05586773 + 1.05285093i.$$

The corresponding $\|\delta\mathbf{w}\|$ values are 0.102659, 1.802944. Fig. 6 (left) shows the resulting curves. The first solution (red curve) is evidently a very reasonable modification of the original curve (blue), preserving its endpoints and end tangents. Although the second solution (green curve) also has this property, it exhibits tight loops — a common feature [20,21] among the multiple solutions to PH quintics that satisfy given constraints — and is discarded based on the large $\|\delta\mathbf{w}\|$ value. The perturbed curves with $\|\delta\mathbf{w}\| \leq 0.25$ for $r = -0.4, -0.3, \dots, 0.3, 0.4$ are shown (red curves) in Fig. 6 (right) together with the two curves (gray) having $\|\delta\mathbf{w}\| = 0.25$, obtained for $r = -0.52962446$ and $r = 0.47220859$.

Choosing the pre-image polynomial defined in Example 5, with Bernstein coefficients

$$\mathbf{w}_0 = (2 - \sqrt{3} - \sqrt{5}) - (1 + 2\sqrt{3})i, \quad \mathbf{w}_1 = 2(1 + \sqrt{5}) - i, \quad \mathbf{w}_2 = (2 + \sqrt{3} - \sqrt{5}) + (2\sqrt{3} - 1)i$$

and the choices $r = -0.5, -0.4, \dots, 0.4, 0.5$, the modified quintic PH curves that preserve endpoints and end tangent directions, and satisfy $\|\delta\mathbf{w}\| \leq 0.25$ are shown (red curves) in Fig. 5 (right) together with the two curves (gray) having $\|\delta\mathbf{w}\| = 0.25$, obtained for $r = -0.59313245$ and $r = 0.60204179$.

6. Modification of PH curve arc lengths

The total arc length S of a planar PH curve $\mathbf{r}(t)$ is intimately related to the norm of its pre-image polynomial $\mathbf{w}(t)$, since

$$S = \int_0^1 \sigma(t) dt = \int_0^1 |\mathbf{w}(t)|^2 dt = \|\mathbf{w}\|^2.$$

The arc length S can be changed by a specified amount $\delta S > 0$ by choosing $\delta\mathbf{w}(t)$ to have the norm $\sqrt{\delta S}$ and to be orthogonal to $\mathbf{w}(t)$, since

$$\int_0^1 |\mathbf{w}(t) + \delta\mathbf{w}(t)|^2 dt = \|\mathbf{w}\|^2 + \|\delta\mathbf{w}\|^2 + 2 \operatorname{Re}(\langle \mathbf{w}, \delta\mathbf{w} \rangle),$$

where $\|\mathbf{w}\|^2 = S$, $\|\delta\mathbf{w}\|^2 = \delta S$, and $\text{Re}(\langle \mathbf{w}, \delta\mathbf{w} \rangle) = 0$ when $\mathbf{w}(t)$ and $\delta\mathbf{w}(t)$ are orthogonal. We focus here on the Legendre representation

$$\mathbf{w}(t) = \sum_{k=0}^m \mathbf{c}_k L_k(t) \quad \text{and} \quad \delta\mathbf{w}(t) = \sum_{k=0}^m \delta\mathbf{c}_k L_k(t)$$

of the pre-image polynomial and its perturbation. Recalling the notation from Section 5.2 we set $\mathbf{c}_k = c_{k,1} + i c_{k,2}$ and form, as in Theorem 1, the real vectors

$$\mathbf{a} = (c_{0,1}, c_{0,2}, c_{1,1}, c_{1,2}, \dots, c_{m,1}, c_{m,2})^T \quad \text{and} \quad \mathbf{g} = \mathbf{a} + \text{sign}(c_{0,1}) \|\mathbf{a}\|_2 (1, 0, \dots, 0)^T. \tag{33}$$

The second through last columns of the $(2m + 2) \times (2m + 2)$ matrix $Q = (q_{j,k})_{j,k=1}^{2m+2}$ defined in terms of \mathbf{a} and \mathbf{g} in (33) by the formula (6) then identify the coefficients of the polynomials

$$\mathbf{b}_k(t) = \sum_{j=0}^m \mathbf{b}_{k,j} L_j(t), \quad \mathbf{b}_{k,j} := q_{2j+1,k+1} + i q_{2j+2,k+1}, \quad k = 1, 2, \dots, 2m + 1,$$

that form the orthonormal basis for degree m complex polynomials orthogonal to $\mathbf{w}(t)$ with norms $\|\mathbf{b}_k\| = 1$, $k = 1, 2, \dots, 2m + 1$. Thus, for any real values $\gamma_1, \gamma_2, \dots, \gamma_{2m+1}$ a perturbation polynomial of the form

$$\delta\mathbf{w}(t) = \sum_{k=1}^{2m+1} \gamma_k \mathbf{b}_k(t) \tag{34}$$

is orthogonal to $\mathbf{w}(t)$ and has norm $\|\delta\mathbf{w}\| = \sqrt{\gamma_1^2 + \gamma_2^2 + \dots + \gamma_{2m+1}^2}$. Thus, by assigning values $\gamma_1, \gamma_2, \dots, \gamma_{2m+1}$ that satisfy

$$\gamma_1^2 + \gamma_2^2 + \dots + \gamma_{2m+1}^2 = \delta S, \tag{35}$$

the perturbed pre-image polynomial $\mathbf{w}(t) + \delta\mathbf{w}(t)$ generates a PH curve with arc length $S + \delta S$.

To ensure that the modified curve has the same endpoints as the given PH curve $\mathbf{r}(t)$, assumed to be in canonical form, $\delta\mathbf{w}(t)$ must also satisfy the condition (28), which can be reduced to the quadratic equation

$$\sum_{j,k=1}^{2m+1} \mathbf{f}_{j,k} \gamma_j \gamma_k + \sum_{k=1}^{2m+1} \mathbf{f}_k \gamma_k = 0, \quad \text{where} \quad \mathbf{f}_{j,k} := \sum_{\ell=0}^m \mathbf{b}_{j,\ell} \mathbf{b}_{k,\ell}, \quad \mathbf{f}_k := 2 \sum_{\ell=0}^m \mathbf{b}_{k,\ell} \mathbf{c}_\ell, \tag{36}$$

in $\gamma_1, \dots, \gamma_{2m+1}$. Eq. (35) and the real and imaginary parts of Eq. (36) constitute a system of three quadratic equations for $2m + 1$ factors $\gamma_1, \dots, \gamma_{2m+1}$ in (34), which allows one to fix $2m - 2$ of them, and then solve the system using Newton–Raphson iterations or some other algebraic solver.

Remark 2. If we denote by Q_R the sub-matrix of Q with rows $1, 3, \dots, 2m + 1$ and columns $2, 3, \dots, 2m + 2$, and by Q_I the sub-matrix of Q with rows $2, 4, \dots, 2m + 2$ and columns $2, 3, \dots, 2m + 2$, and we define the complex matrix $\mathbf{Q} = Q_R + i Q_I$, the vector $\delta\mathbf{C}$ of the coefficients of $\delta\mathbf{w}$ can be expressed as $\delta\mathbf{C} = \mathbf{Q} \boldsymbol{\gamma}$ for $\boldsymbol{\gamma} = (\gamma_1, \gamma_2, \dots, \gamma_{2m+1})^T$, which gives a more compact representation of (36), namely

$$\boldsymbol{\gamma}^T \mathbf{F} \boldsymbol{\gamma} + 2 \boldsymbol{\gamma}^T \mathbf{Q} \mathbf{C} = 0, \quad \mathbf{F} := \mathbf{Q}^T \mathbf{Q}.$$

Example 7. Consider the PH quintic specified by the pre-image polynomial in Example 6, with arc length $S = 1.23740482$. The complex matrix \mathbf{Q} , defined in Remark 2, is

$$\mathbf{Q} = \begin{bmatrix} 0.048391 + 0.998792i & 0 & 0 & -0.148557 + 0.003707i & -0.305920 + 0.007634i \\ 0 & 1 & i & 0 & 0 \\ 0.003707 + 0.007634i & 0 & 0 & 0.988619 - 0.023436i & -0.023436 + 0.951738i \end{bmatrix}.$$

The perturbation $\delta\mathbf{w}(t)$ in (34) is expressed in terms of the five parameters $\gamma_1 \dots, \gamma_5$. Fixing two of them and choosing $\delta S = 0.01$, the remaining parameters may be computed as the solution of Eqs. (35)–(36). For $\gamma_4 = \gamma_5 = 0$ four solutions are identified:

$$\begin{aligned} (\gamma_1, \gamma_2, \gamma_3) &= (0.0047585271, \pm 0.074073623, \mp 0.067010856), \\ (\gamma_1, \gamma_2, \gamma_3) &= (-0.0047585271, \pm 0.074073623, \pm 0.067010856). \end{aligned}$$

Fixing $\gamma_2 = \gamma_3 = 0$ the system has only two solutions:

$$\begin{aligned} (\gamma_1, \gamma_4, \gamma_5) &= (-0.032364637, 0.094555975, 0.0034202026), \\ (\gamma_1, \gamma_4, \gamma_5) &= (0.030467676, -0.094859055, 0.0085720767). \end{aligned}$$

Using these values, the Legendre coefficients of $\delta\mathbf{w}(t)$ follow from $\delta\mathbf{C} = \mathbf{Q} \boldsymbol{\gamma}$. The resulting PH quintics with increased arc length, generated by the modified pre-image polynomials $\mathbf{w}(t) + \delta\mathbf{w}(t)$, are shown in Fig. 7.

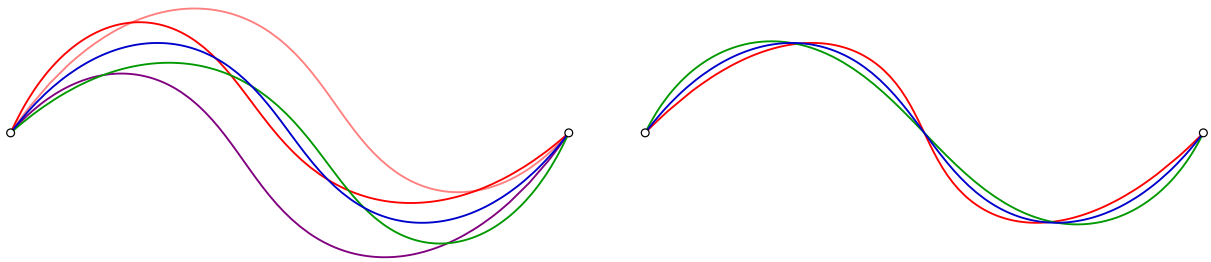


Fig. 7. The PH quintic from Example 6 (blue), together with PH quintics (different colors) with arc lengths increased by $\delta S = 0.01$, sharing the same endpoints, computed by fixing $\gamma_4 = \gamma_5 = 0$ (left) and $\gamma_2 = \gamma_3 = 0$ (right).

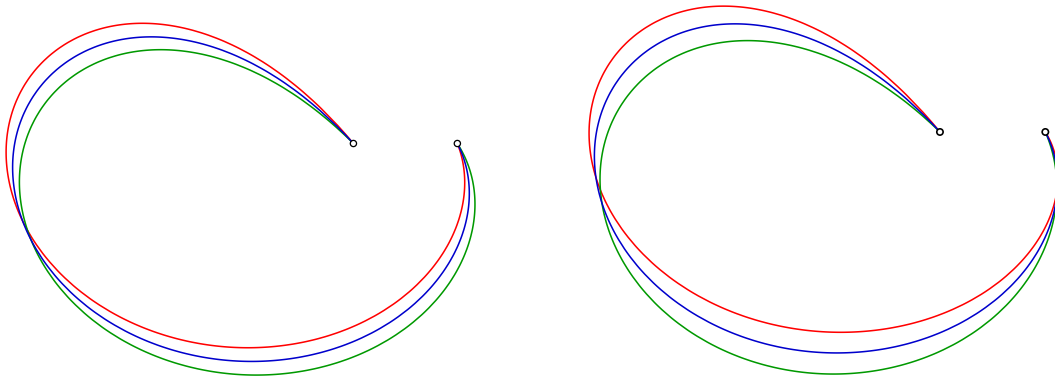


Fig. 8. The PH quintic from Example 8 (blue), together with PH quintics (red, green) with arc lengths increased by $\delta S = 0.01$, sharing the same endpoints, computed by fixing $\gamma_4 = \gamma_5 = 0$ (left) and $\gamma_2 = \gamma_3 = 0$ (right).

Example 8. As a final example, we choose the PH quintic specified by the pre-image polynomial in Example 5, with arc length $S = 11$, and follow the same steps as in the previous example. For the choice $\delta S = 0.01$ and $\gamma_4 = \gamma_5 = 0$ there are two solutions,

$$\begin{aligned}
 (\gamma_1, \gamma_2, \gamma_3) &= (-0.068622784, 0.069792544, -0.020491812), \\
 (\gamma_1, \gamma_2, \gamma_3) &= (0.068681604, -0.069717905, 0.020548745),
 \end{aligned}$$

shown in Fig. 8 (left). Fixing $\gamma_2 = \gamma_3 = 0$, we obtain

$$\begin{aligned}
 (\gamma_1, \gamma_4, \gamma_5) &= (-0.034621641, -0.083559293, -0.042651924), \\
 (\gamma_1, \gamma_4, \gamma_5) &= (0.031439019, 0.083161950, 0.045778578).
 \end{aligned}$$

The corresponding curves are shown in Fig. 8 (right).

7. Closure

Interpreting planar polynomial curves as complex-valued functions of a real parameter $t \in [0, 1]$ facilitates the introduction of an inner product, norm, and metric function that permit measurement of curve magnitudes and of the distances and angles between curves. The concept of orthogonal curves is then possible, leading to a procedure to construct a basis spanning all planar curves that are orthogonal to a given planar curve.

These concepts were applied to the complex pre-image polynomials that define planar Pythagorean-hodograph (PH) curves, to develop schemes that allow bounded modifications of a given PH curve, without compromising its PH nature. Specializations of these schemes that accommodate the preservation of curve endpoints and end tangents have also been presented, and the use of an orthogonal basis for a given PH curve pre-image polynomial to achieve a desired change in the arc length of the PH curve was demonstrated.

The methodology presented herein may also be generalized to the planar Pythagorean-hodograph splines [22] or to the spatial Pythagorean-hodograph curves through the quaternion representation [14,15], and preliminary results have already been reported in [23]. A further domain of interest concerns the possible adaptation of the methodology from curves to parametric surfaces, defined as vector quaternion polynomial functions of two parameters over triangular or rectangular domains.

Data availability

The data are described in the manuscript.

Acknowledgments

The second and the fourth authors have been partly supported by the research program P1-0288 and the research grants N1-0137, N1-0237 and J1-3005 by the Slovenian Research and Innovation Agency. The third author has been partly supported by the research program P1-0404 and the research grants N1-0296, N1-0210 and J1-4414 by the Slovenian Research and Innovation Agency.

References

- [1] R.T. Farouki, The conformal map $z \rightarrow z^2$ of the Hodograph plane, *Comput. Aided Geom. Des.* 11 (1994) 363–390.
- [2] R.T. Farouki, T. Sakkalis, Pythagorean Hodographs, *IBM J. Res. Develop.* 34 (1990) 736–752.
- [3] R.T. Farouki, *Pythagorean–Hodograph Curves: Algebra and Geometry Inseparable*, Springer, Berlin, 2008.
- [4] H. Alt, C. Knauer, C. Wenk, Comparison of distance measures for planar curves, *Algorithmica* 38 (2004) 45–58.
- [5] G. Rote, Computing the Fréchet distance between piecewise smooth curves, *Comput. Geom.* 37 (2007) 162–174.
- [6] E. Vodolazskiy, Discrete Fréchet distance for closed curves, *Comput. Geom.* 111 (2023) 101967.
- [7] T. Lyche, K. Mørken, A metric for parametric approximation, in: *Curves and Surfaces in Geometric Design*, Chamonix-Mont-Blanc, 1993, 1994, pp. 311–318.
- [8] R.T. Farouki, F. Pelosi, M.L. Sampoli, Construction of planar quintic Pythagorean-Hodograph curves by control-polygon constraints, *Comput. Aided Geom. Des.* 103 (2023) 102192.
- [9] S.H. Kim, H.P. Moon, Rectifying control polygon for planar Pythagorean Hodograph curves, *Comput. Aided Geom. Des.* 54 (2017) 1–14.
- [10] H.P. Moon, S.H. Kim, S.H. Kwon, Shape analysis of planar PH curves with the Gauss–Legendre control polygons, *Comput. Aided Geom. Des.* 82 (2020) 101915.
- [11] Z. Šir, Classification of planar Pythagorean Hodograph curves, *Comput. Aided Geom. Des.* 80 (2020) 101866.
- [12] R.T. Farouki, Identifying Pythagorean–Hodograph curves closest to prescribed Bézier curves, *Comput. Aided Des.* 149 (2022) 103266.
- [13] E. Kreyszig, *Introductory Functional Analysis with Applications*, Wiley, New York, 1989.
- [14] H.I. Choi, D.S. Lee, H.P. Moon, Clifford algebra, spin representation, and rational parameterization of curves and surfaces, *Adv. Comp. Math.* 17 (2002) 5–48.
- [15] R.T. Farouki, M. al Kandari, T. Sakkalis, Structural invariance of spatial Pythagorean Hodographs, *Comput. Aided Geom. Des.* 19 (2002) 395–407.
- [16] R.T. Farouki, M. Knez, V. Vitrih, E. Žagar, Spatial C^2 closed loops of prescribed arc length defined by pythagorean Hodograph curves, *Appl. Math. Comput.* 391 (2021) 125653.
- [17] C. Zwikker, *The Advanced Geometry of Plane Curves and their Applications*, Dover Publications (reprint), New York, 1963.
- [18] R.T. Farouki, The Bernstein polynomial basis: a centennial retrospective, *Comput. Aided Geom. Des.* 29 (2012) 379–419.
- [19] R.T. Farouki, Legendre–Bernstein basis transformations, *J. Comput. Appl. Math.* 119 (2000) 145–160.
- [20] R.T. Farouki, C.A. Neff, Hermite interpolation by Pythagorean–Hodograph quintics, *Math. Comput.* 64 (1995) 1589–1609.
- [21] R.T. Farouki, Construction of G^1 planar Hermite interpolants with prescribed arc lengths, *Comput. Aided Geom. Des.* 46 (2016) 64–75.
- [22] G. Albrecht, C.V. Beccari, J.-C. Canonne, L. Romani, Planar Pythagorean–Hodograph B-spline curves, *Comput. Aided Geom. Des.* 57 (2017) 57–77.
- [23] R.T. Farouki, C. Stoppato, Spatial pythagorean Hodograph curves with identical arc lengths generated by rotations of quaternion polynomials, 2024, preprint.